 doi:10.20944/preprints202107.0309.v1

Article

Entropy and Entropic Forces to Model Biological Fluids

Rafael M. Gutierrez [1,2,*], George T Shubeita [1], Chandrashekhar U. Murade [1] and Jianfeng Guo [1]

[1] New York University Abu Dhabi; rmg2165@nyu.edu, geroge.shibeita@nyu.edu, Chandra.murade@nyu.edu, dannyguo@nyu.edu
[2] Universidad Antonio Nariño; director.sistemas.complejos@uan.edu.co
* Correspondence: rmg2165@nyu.edu

Abstract: Living cells are complex systems that may be characterized by fluids crowded by hundreds of different elements in particular by a high density of polymers; they are an excellent and challenging laboratory to study exotic emerging physical phenomena where entropic forces emerge from organization processes of many-body interactions. The competition between microscopic and entropic forces may generate complex behaviors like phase transitions that living cells may use to accomplish their functions. In the era of the big data, when biological information abounds but general principles and precise understanding of the microscopic interactions scarce, the entropy methods may offer significant information. In this work we develop a model where the thermodynamic equilibrium results from the competition between an effective electrostatic shortrange interaction and the entropic forces emerging in a fluid crowded by different size polymers. The target audience for this article are interdisciplinary researchers in complex systems, particularly in thermodynamics and biophysics modeling.

Keywords: entropic forces; biological fluids; crowding; polymer's configurations.

1. Introduction

The biological fluids, inside living cells, are crowded by a diversity of polymers as chains made of monomers from 1.5 to 7Å length, as DNA is made of nucleotides. The diversity of polymers in a biological fluid may have different configurations depending on their length, temperature, solvent and crowding [1,2]. Some simple models are useful and powerful but they may not account for specific details that eventually become dominant effects. For example, emergent medium and long-range entropic forces may cause polymer compression but electrostatic short-range forces cause polymer stretching generating a resourceful competition of forces with nonobvious behaviors and consequences. The outcome of these competing forces strongly depends on small variations of the specific circumstances such solvent, the nature and size of the polymers involved and the crowding they generate to the other polymers and to themselves.

The quality of the solvent depends on both the chemical compositions of the polymer and the kind of solvent molecules. If a solvent has the precise characteristics to cancel the effects of excluded volume expansion or compression, depending on the point of view, the polymer chain will behave exactly as predicted by the random walk or ideal chain model. At short range, the steric effects are nonbonding interactions that influence the configuration and reactivity of all ions and molecules of the fluid. Steric effects complement and can be considered part of the electrostatic shortrange intrapolymer and interpolymer interactions, between monomers from the same polymer and monomers from different polymers, dictating the shape and reactivity of polymers [1-4].

Such richness and complexity of biological fluids allow sophisticated dynamics depending on subtle changes of the internal and environmental parameters including temperature in a constant feedback. Therefore, the effects of entropy are ubiquitous in biological fluids, in fact it is indispensable for certain emergent properties from the ordering and self-ordering processes that give life to inert matter as an emergent quality from the

 doi:10.20944/preprints202107.0309.v1

complexity of many interacting simple and not living but very dynamic and sensitive constituents. The ordering power of entropic forces emerges from the tendency of thermodynamic systems to maximize its entropy understood as a tendency to disorder, but towards more probable states. Understanding complexity to develop simple models, capture the essentials transforming the complication of diversity into the power of organization [2-5]. In this work we model the complexity of a biological fluid by describing the polymer configuration changes by means of two competing and complementary forces: an expanding short-range force F_1 accounting for electrostatic forces, electronic clouds superpositions and quantum exclusion principle among others, and a medium and long-range compressive force F_2 accounting for entropic forces like polymer packing, clustering and osmotic pressure among others. These two resulting effective forces shape the configuration of the polymer and therefore the activity and effects of the molecules, also depending on temperature as a complex thermodynamic system.

The traditional measures of polymer configurations are the hydrodynamic radius R_h, obtained from experimental viscosity measures and quasi-elastic light scattering; the radius of gyration R_g, obtained from experimental measures of small angle X-ray scattering and; the end-to-end distance Re-e, obtained from Fluorescence Resonance Energy Transfer, FRET, among other techniques. In certain particular conditions these three different measures have some theoretical approximations and relations. For good solvents $R_h \approx 5/3\ R_g$ and $R_g \approx 1/\sqrt{6}\ R_{e\text{-}e}$. For example, large nonionic polymers like polyethylene glycol, PEG, of molecular weight 6kg/M, are constituted by a little less than one hundred monomers with a $R_h \approx 24$Å or $R_g \approx 40$Å at standard biological fluid conditions [5-8]. On the other hand, small but charged polymers, polyelectrolytes, made of a few monomers, for example a short single strand of DNA of the nucleotide or base T (thymine), pT, may have R_g of a few to 100Å, depending on the crowding, number of monomers and solvent. Therefore, the size, shape and compactness of polymer configurations may give very different results for the corresponding measures obtained with different techniques [9], depending on small variations of the conditions Theoretically, the competition of a negative short-range expanding force F_1, and a positive large range compressing force F_2, is well described by a Lenard-Jones-like potential, $V_{L\text{-}J}$. For a small pT embedded in a fluid crowded by large PEGs, for example, the minimum of the $V_{L\text{-}J}$ indicates the thermodynamic equilibrium of the system, when the pTs have specific values of R_g, R_h and $R_{e\text{-}e}$ as the forces F_1 and F_2 work to mold its size and shape defining its folding and unfolding properties. The crowding, measured by the percentage or density of large polymers, does not have to be very high, 20% is considered standard for biological fluids with small polyelectrolytes and large nonionic polymers. Small and charged polymers like a small pT, has a characteristic stiffness, represented by F_1 as it is mainly the repulsion force between the negatively charged monomers that constitutes the charged DNA backbone. In contrast, F_2 includes crowding, the reduction of available volume that effectively increases the concentration of macromolecules and generate an osmotic pressure upon themselves and over the other constituents of the biological crowded fluid. Therefore, the shape of a pT depends on the feedback of these two forces. The different ranges of these two forces result in subtle balances, when the intensity of one increases the intensity of the other decreases and vice versa as the pT changes its configuration, and consequently, changes the results of the measures and their quantitative relations.

This work is divided in four sections: Section 2 presents the theoretical framework, section 3 presents the model calculations and compare experimental and theoretical results, in sections 4 the results are discussed and analyzed and, finally, in section 5 are presented some conclusions and perspectives.

2. Framework and Methods

A polymer is a complex system with many different possible configurations that may be characterized by their size and shape. The most desirable characteristics are those that may be verified experimentally, directly or indirectly, and also can be experimentally

controlled such as the length of the polymer and the solvent and crowding concentrations. Crowding of biological fluids seems to be indispensable for living functions within the cell and among the living cells [1-3]. RNA and DNA are confined, packed, twisted, and pulled on, depending on their polymeric properties as polyelectrolytes or charged polymers. Their conformation, folding and flexibility strongly depends on ionic solution conditions.

The configurations of a polymer can be measured in different ways. The hydrodynamic radius R_h, is experimentally measurable using the diffusion coefficient corresponding to the model of hydrated polymer molecules as solid spheres with radius R_h using the Einstein viscosity relation. The root-mean-squared end-to-end distance of a polymer is denoted by $R_{e\text{-}e}$, which in standard conditions is $R_{e\text{-}e} \approx 3.1Rh$ [6], for a freely jointed chain when $\nu = 1/2$ we can write $Re\text{-}e = 6^{1/2}R_g = A_0 (6N)^{1/2}$ where N is the number of monomers and A_0 can be interpreted as the effective length of one monomer and, for an ideal chain $R_{e\text{-}e} = N^{1/2}l$ where l is the Kuhn or persistent length [10]. In general, it is considered the scaling relation $R_{e\text{-}e} \sim N^{\nu}$ where the scaling factor $\nu = 3/5 = 0.6$ corresponds to a good solvent, for a sphere $\nu = 0.33$, for theta solvent $\nu = 0.5$ and $\nu = 1$ for a straight rope-like polymer. A good solvent generates a pair-wise repulsion for a full chain swelling, on the other hand a regular solvent does not generate repulsion and the chain collapses, closer to a hard sphere. Therefore, increasing salt concentration in water a solvent for a polyelectrolyte like a pT, acts as bad solvent because it reduces the pair-wise repulsion between the charged monomers of the pT by ionic screening making the polyelectrolyte softer and easer to compress into compact configurations by any force that may be present. This is contrary to a good solvent that in general is considered a substance that increases the stiffens of the polymers to favor the stretched configurations, not the collapsed configurations towards a compact sphere, corresponding to low salt concentrations in the case of polyelectrolytes such as a pT.

The radius of gyration R_g, is obtained from angular inertia. Accounts for how the mass of an object is distributed about its center of mass. It can be expressed as $R_g = A_0 N^{\nu}$ where N is the number of monomers, A_0 is the size or effective length of a monomer and ν measures the stiffness of the polymer, both depending on salt concentration and are experimentally measured for some polyelectrolytes [7]. From experimental data R is chosen equal to R_h which is experimentally measurable. For good solvents R_h and R_g may be significantly different. R_g is a model-free measure of the global size of a polymer, it can be directly determined from small angle X-ray scattering SAXS [8,11,12]. As already mentioned, the dependence of R_g on the number of bases or monomers, N, is well described by a general scaling law of the form $R_g = A_0 N^{\nu}$ [13], with the values of A_0 and ν well estimated for pT of small N at different concentrations of salt [7]. In the extreme case where $\nu = 1$, the molecular size scales linearly with the number of monomers, suggesting that the monomers in the polymer are rigidly connected, as in the case of a single-stranded DNA on short length scales, ssDNA. A smaller value of ν indicates greater molecular flexibility; in the limiting case where the polymer behaves as a self-avoiding random walk (SAW) chain, it corresponds to $\nu = 0.588$ for large N [13]. The steric contribution is included in A0 and ν even if it may or may not depend on salt concentration. Therefore, R_g is a good measure of the size of a small pT experimentally measurable, it must be a function of salt (NaCl) concentration s, of the number of monomers N and of the crowding in percentage P, of mass or volume of the fluid. Then, we can write:

$$R_g(s, N, P) = A_0(s) N^{\nu(s)} F(s, N, P) \ , \tag{1}$$

where the first two factors of the right-hand side of the equation have the information of the pT without crowding and $F(s,N,P)$ is the deformation factor representing the effects of crowding which also depends on s and N and obviously of P. By definition $F(s,N,0) \equiv F_0 = 1$ when P=0. In the absence of long-range interactions, the following mean values relation holds, $R_g^2 = 1/6\ R_{e\text{-}e}^2$.

Preprints (www.preprints.org) | NOT PEER-REVIEWED | Posted: 13 July 2021 doi:10.20944/preprints202107.0309.v1

The contour length of a polymer is given by $L = NA_0$, is the polymer stretched by pulling its ends apart. The Kuhn length or persistent length l, defines the stiffness of the polymer, is the length of n rigid monomers before the polymer bends, smaller for softer monomers. The corresponding values of A_0 and ν depending on s for a pT are presented in table 1, obtained from experimental data [7]. The experimental data can be fitted to the following expression and then obtain extrapolated values of A_0 and ν for all possible and also idealized theoretical very high concentration values of s:

$$A_0 = 11/4 + y/4 \text{ and } \nu = 0.794 - 0.0674y\ , \quad (2)$$

where $y = log10\ s$, $0 < y \leq 3$ and $0 < s \leq 20M$ is the salt concentration. However, accordingly to the experimental results, A_0 has not a clear tendency as a function of s but a strong variability for some particular values of s. Therefore, for the sake of qualitative estimates throughout this work, $A_0(s)$ is normalized to 1 for all values of s. This normalization gets rid of noisy effects at monomer scale and allows to capture essential features at polymer scale.

Table 1. Experimental data and extrapolated values using equation 2, for the parameters A_0 and ν as functions of $0 < s \leq 20$M. The experimental values of $\nu(s)$ as a function of s are accurate and well fitted to the corresponding equation 2, to be used for comparison of experimental and theoretical estimates of R_g. In contrast the values of $A_0(s)$ indicated in the table, are a linear extrapolation with large and inconsistent deviations from experimental measurements. Therefore, the experimental values are not used in this work and it is set $A_0(s)=1$ for all values of s.

Salt [s]= *mM*	1mM	12.5	25	125	225	525	1M	10M	20M
$A_0(s)$	2.750	3.024	3.100	3.274	3.38	3.430	3.500	3.750	4.900
$\nu(s)$	0.794	0.720	0.700	0.653	0.636	0.607	0.592	0.524	0.504

The microscopic forces and their interplay constituting F_1 is very complex, including the van der Waals interaction that may change by environmental chemical bonds, temperature increases exclusion volume because of random walk and vibrations, steric effects correspond to very short-range but nonbonding interactions like repulsive forces between overlapping electron clouds, attraction by Casimir effect become repulsive at certain distance by electron clouds overlapping, among other microscopic complexities of F_1. However, all of them strongly depend on microscopic charge distributions and therefore can be reduced or summarized into an electrostatic force strongly dependent on the ion's concentration provided by the solvent. Then the solvent characteristics represented by salt concentration can be directly related with the polymer stiffness as the emergent relevant quality at the relevant scales of the $V_{L\text{-}J}$. Thus, through the effective forces F_1 and F_2, the model brings up an effective potential from microscopic interactions and entropic forces emergent from the complexity of the system.

Macromolecular crowding is an effect exerted by large molecules on the properties of other large molecules and indirectly to themselves and finally to all the other molecules contained in the biological fluid, depending on the crowding percentage of the total mass or volume of the fluid. In summary, F_1 and F_2 result in polyelectrolytes less or more flexible, with configurations sometimes difficult to explain in terms of experimental measurements, but they do not collapse to globular forms for large ranges of salt concentration [7]. Electrostatic repulsion tends to disfavor compaction and folding towards a rope-like configuration. Size decreases with increasing salt concentration because the electrostatic repulsion is increasingly screened by salt ions. However, even for high salt concentrations

 doi:10.20944/preprints202107.0309.v1

of 1M, the pT does not collapse into globular forms, indicating that entropic forces are neutralized at some point by other forces like friction, viscosity and thermal fluctuations as macroscopic expressions of F_1. Since water, H2O, with NaCl, *s*, generates $^{+}$Na ions screening the negative charge of polyelectrolytes, increasing s decreases the stiffness of the polyelectrolyte generated by negative charge repulsion between the constituent monomers, changing the polymer configuration to a more spheroid like shape from a more stretched rope-like configuration.

Since the osmotic pressure is an effect of large polymers on polymers of similar size, the osmotic pressure on small pTs will be more effective with smaller PEGs for the same volume percentage of crowders; smaller crowders may be better [3]. More precisely, polymers are better crowders for similar size polymers. In addition, the shape of the polymers is important to increase the effective surface of interaction. When the polymers are small, they no longer can be well approximated by hard spheres, but by soft spheres with changes of symmetry and even dimensionality, that can be detected and eventually quantified from the experimental measures R_h, R_g and $R_{e\text{-}e}$. For soft spheres, the work of the forces F_1 and F_2 generate small changes of configurations absorbing or releasing some energy towards a thermodynamic equilibrium different from that of hard spheres and, in such conditions, the relation of the two forces may change and the small polymers can eventually stretch under increasing crowding. Therefore, the thermodynamic equilibrium is the result of a processes at different scale ranges that can be represented by the interplay of the two effective forces F_1 and F_2 very sensitive to the specific conditions of solvent, size of the polymers, crowding and temperature.

The two resulting effective forces F_1 and F_2 can be represented by a Lennard-Jones-like potential, $V_{L\text{-}J}$:

$$V_{L-J}(r) = a\varepsilon\left[\left(\frac{\sigma}{r}\right)^m - \left(\frac{\sigma}{r}\right)^n\right] \tag{3a}$$

or

$$V_{L-J}(r) = \varepsilon\left[\left(\frac{r_m}{r}\right)^m - b\left(\frac{r_m}{r}\right)^n\right]. \tag{3b}$$

Traditionally, r is the distance between two interacting particles, ε is the depth of the potential well, and σ is the distance at which the particle-particle potential energy is zero, and has its minimum at a distance r_m, where the potential energy has the value $-\varepsilon$. The interpretation in this work for r is not the distance between two particles but the size of the pT that changes under the pressure of the PEG. The reference point is one extreme of the pT and r is the distance to the other extreme, then $r_m = (m/n)^{1/m-n}\sigma$ represents the compression or expansion of the pT under the two competing forces. The condition $m > n$ represents the short- and long-range forces respectively. The system with large polymers PEG, and a small polyelectrolyte, pT, is depicted in figure 1 with the corresponding $V_{L\text{-}J}$. Under this condition m and n can have many different values compared to the most common and original Lennard-Jones potential's values m= *12* and n=*6*. The forces F_1 and F_2 are given by the variation of the potential where negative indicates repulsive and positive indicates attractive force, or stretching and compressing the pT respectively:

$$\frac{-dV_{L_J}(r)}{dr} = -F_1(r) + F_2(r). \tag{4}$$

Preprints (www.preprints.org) | NOT PEER-REVIEWED | Posted: 13 July 2021 doi:10.20944/preprints202107.0309.v1

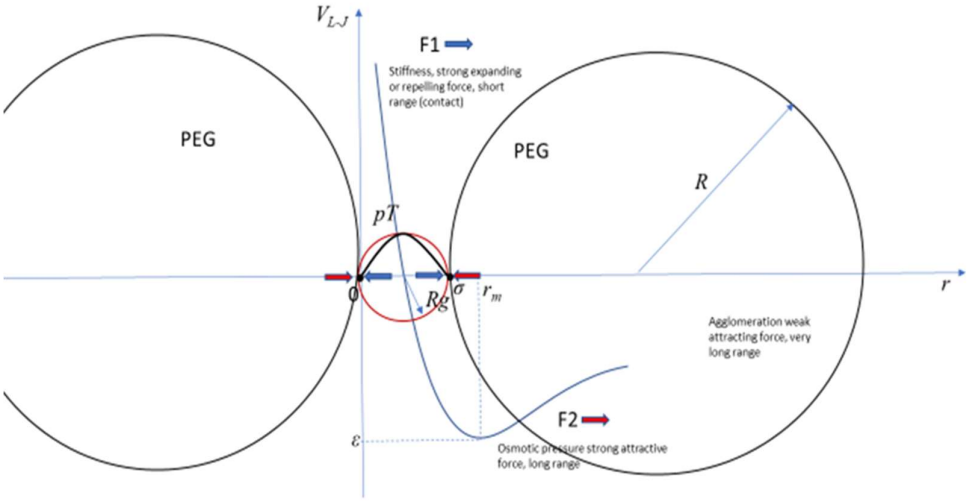

Figure 1. A general Lenard-Jones-like potential representing the forces F1 and F2 in a system of a small polyelectrolyte pT under the pressure of large nonionic polymers PEG.

From equations 3 a and b, the equilibrium of the system is different depending on *s*, *N* and *P* which define the relations between the two forces, determined by:

$$r_m = \left(\frac{m}{n}\right)^{1/(m-n)} \sigma \tag{5}$$

Different values of the relative intensities and ranges of the two forces represented by m and n, correspond to specific values of *a* and *b* and a quantitative relation between r_m and σ. The factor F_{mn}:

$$F_{mn} = \left(\frac{m}{n}\right)^{1/(m-n)} \tag{6}$$

measures the contraction of the pT, proportional to its length when there is not crowding. When $F_{mn} > 1$ the pT is compressed and when $F_{mn} < 1$ the pT is stretched and in both cases the configuration of the polyelectrolyte is changed at the same time that it changes the effects of the two forces upon itself.

From the diagram of the $V_{L\text{-}J}$ and the corresponding definitions, we identify $R_{e\text{-}e}=\sigma$ and $r_m = \beta\sigma = \alpha R_{e\text{-}e}$ where β is the measure of change of size of the pT under the osmotic pressure from crowding; $R_{e\text{-}e}=\sigma$ is the size of the compressed pT and $r_m = \beta\sigma = \beta R_{e\text{-}e}$ is the measure of the pT without crowding. This approximation is theoretically valid for any other configuration of the pT considering that $R_{e\text{-}e}$ measures the characteristic size of the pT and its extremes tend to the surface of the volume defined by the polymer as the statistically more probable locations for them. Therefore, the compression factor depends on the number of monomers constituting the pT, *N*, the salt concentration *s*, and the crowding percentage, *P*, given by:

$$\beta(s, N, P) = \left(\frac{m}{n}\right)^{\frac{1}{m-n}} \tag{7}$$

Preprints (www.preprints.org) | NOT PEER-REVIEWED | Posted: 13 July 2021 doi:10.20944/preprints202107.0309.v1

From equations 5 to 7 we get $a= \beta m$ and $b=\beta m-n$. For example, for a pT approximated by an ellipsoid instead of a sphere (the ellipsoid of higher symmetry), from equations 3 and 4 at thermodynamic equilibrium, the forces F_1 and F_2 must have the approximated relation given by:

$$F_1 = F_2\left(1 - \frac{2d}{\sqrt{d^2+c^2}}\right), \quad (8)$$

where d is the largest axes and c the other two equal and smaller axes of the ellipsoid. In the case of a sphere when $c=d$, we obtain $F_1 = -0.41F_2$, and for an ellipsoid with $c=d/2$ we obtain $F_1 = -0.78F_2$. These simple calculations show the changes that the feedback between the pT geometry and the forces can produce on the configurations of the pT. For larger F_1 relative to F_2, the configuration of the pT tends to loss symmetry from a sphere to an ellipsoid. Since F_2 represents a pressure homogeneously distributed over the surface of the pT, the relation between the vertical and horizontal components changes when the pT losses symmetry, then the effects enhance itself and the ellipsoid gets still flatter, changing the relation $R_{e\text{-}e}/R_g$ that can be measured experimentally.

Since the entropic forces are isotropic, in general they are a compression or compacting force upon the pT, but the monomers of the extremes of the pT have more degrees of freedom than the other monomers and then they tend to walk away from the others towards the surface of the volume occupied by the polymer, as a more probable configuration. In contrast, F_1 is directional and tends to stretch the polymer towards a more elongated and less spherical and symmetric configuration that also generates a positive feedback with F_2 to make the pT configuration still less symmetric and flatter, tending to reduce dimensionality from 3D to 2D towards a parabola or horseshoe like configuration and finally to the extreme 1D configuration of a stretched rope. For smaller pTs, this tendency to dimensionality reduction generated by the feedback of the forces and the geometry of the pT is stronger.

The idealized configurations corresponding to different stages of symmetry and dimensionality loss may be the following:

1- Rope like shape: is the maximum extended idealized configuration with all the monomers in line with the extremes maximally separated from each other. It is the dominant tendency of a strongly charged polyelectrolyte with strong repulsion between monomers, a very stiff polymers difficult to bend. It is an almost 1D configuration. Its total length will be approximately equal to $R_{e\text{-}e}(s,p)=A_0(s)N$.

2- Parabola or horseshoe-like shape: is a less extended configuration still dominated by F1 repulsion among monomers but weakened by the larger distance between the extreme monomers, the polymer is still stiff but the entropic packing force becomes relatively more important and the extreme monomers can get closer bending the polymer. Compared with the rope like shape the dimensionality increases to almost 2D. Its total length is still approximately equal to $A_0(s)N$ but $R_{e\text{-}e}(s,N)$ has a more complex dependency on s and N.

3- Ellipsoid shape: when the polymer is soft and longer the entropic packing force makes the monomers tend to fill more homogenously the space between the two extremes defining an elongated volume. The extremes still tend to be at the end of the longer axes of the elongated shape because it is where they have less constraints and maximum probability to be. Its dimensionality increases to 3D.

4- Spheroid shape: when the polymer is still softer and longer the entropic packing force makes the monomers to homogeneously fill the space between the extremes but with maximum symmetry because the preferred directions defined by the interactions

Preprints (www.preprints.org) | NOT PEER-REVIEWED | Posted: 13 July 2021 doi:10.20944/preprints202107.0309.v1

between monomers lose importance but the extremes stay close to the surface for the same entropic reasons mentioned before. The spherical symmetry of the volume occupied by the monomers becomes definitely 3D, however. The monomers can be more or less disperse in the spheroid volume occupied by the polymer tending to a compact and solid sphere. When the compression force F_2 overcomes the expansion force F_1, the volume occupied by the monomers becomes more and more symmetric and asymptotically tending to the most compact and further incompressible configuration limited by temperature and steric interactions between monomers; larger polymers always have more room for compression. For a compact sphere $R_{e\text{-}e} \sim 2R_g$.

Theoretically and formally, the radius of gyration, R_g, is defined as the mean square distance of the monomers to the center of mass of the polymer:

$$R_g = \left(\frac{1}{N}\sum_{i=1}^{N} r_i^2\right)^{\frac{1}{2}}, \tag{9}$$

where N is the number of monomers and r_i is the distance from the i-th monomer to the center of mas of the polymer, considering all the monomers with mass equal to one.

As indicated previously, the radius of gyration R_g has been measured for different values of s and N with $P=0$ following the scaling relation [6]:

$$R_g(s, N, 0) = A_0(s)N^{\nu(s)}. \tag{10}$$

Defining α(s,p) as $R_g = \alpha R_{e\text{-}e}$, the proportionality factor between these two measures of a polymer, some theoretical and experimental limits can be compared to understand better the changing configurations of a pT under changes of s, N and P causing changes of F_1 and F_2. For high values of s the pTs can be considered freely jointed polymers, i.e. stochastic chains in 3D with $\alpha \approx 1/\sqrt{6} \approx 0.408$, following a random walk in 3D in the absence of any force: $F_1=F_2=0$. Different values of α indicate how different the corresponding polymer configuration is compared to that of the freely jointed polymer.

When the monomers are considered hard spheres with no electrical charge of any kind, $F_1=0$, and no crowding but with interpolymer entropic force, packing force, which means F_2 weak, the polymer tends to a symmetric spheroid 3D volume randomly occupied as a tight random walk of the monomers, with the extremes tending to the surface by the entropic reason explained above. Depending on the temperature T, the spheroid may be more or less compact tending to a dense and solid sphere for very low T. In such conditions the polymer can be well approximated by a solid sphere of radius R with $R_g=(6/5)^{1/2}R \approx 1.1R$ corresponding to the mathematical ideal radius of gyration of a solid sphere with radius R obtained from the corresponding 3D gyration tensor. If we estimate R by making the volume of N solid spheres of unit radius equal to the volume of a solid sphere of radius R we obtain $R \approx \sqrt[3]{N}$ then, for a polymer made of N monomers with a compact sphere configuration we obtain $R_g \approx (6/5)^{1/2}N^{1/3} \approx 1.1N^{1/3}$ indicating that the radius of gyration is 10% larger than the radius of the sphere. Considering the entropic tendency of the extremes of the polymer to be in diametral opposite sides of the sphere, the end-to-end distance would be given by,

$$R_{e-e} \approx 2R = 2N^{\frac{1}{3}} = 2\sqrt{\frac{5}{6}}R_g = 1.8R_g \tag{11}$$

for a solid sphere polymer configuration of N monomers. For a ring-like and a disc-like tight and idealized configurations of N monomers $R_g \approx \sqrt{2N}$ and $R_g \approx N$ respectively.

Preprints (www.preprints.org) | NOT PEER-REVIEWED | Posted: 13 July 2021 doi:10.20944/preprints202107.0309.v1

In order to estimate R_g for different configurations and be able to compare values of R_g and $R_{e\text{-}e}$ to obtain more information about the actual configurations of a real polyelectrolyte under the forces F_1 and F_2 with different conditions of the parameters *s, N* and *P*, we use a second theoretical expression for R_g, resulting from the "wormlike" chain model:

$$R_g = \left[\frac{lL_p}{3} - L_p^2 + \frac{2L_p^3}{l} - \left(\frac{2L_p^4}{l^2}\right)\left(1 - e^{-l/L_p}\right)\right]^{1/2} \quad (12)$$

where L_p is the persistent length, l=N is the contour length with N the number of monomers and the effective monomer length equal to one. With this model we can estimate R_g for polymers of different sizes and with different levels of stiffness. For the maximum stiffness, $L_p \sim N$, and a very large polymer, $N \to \infty$, we obtain $R_g \approx N/4$, which is the same result for the minimum and maximum stiffness of very small polymers, $N \to 1$, because $L_p \to N \to 1$; meaning that small polymers are simple and do not have much room for stiffens variability, it is always close to the maximum, $L_p \approx 1$. The minimum stiffness $L_p = 1$, for very large polymers, $N \to \infty$, gives $R_g \to (N/3)^{1/2}$.

In the following section, we calculate and compare the results of R_g for the two theoretical estimates: the mean square distance to center of mass and the wormlike chain model, equations 9 and 13 respectively, with the experimental approximation estimated from equation 10. These results allow us to compare the geometry of the configurations generated by the correspondent stiffness represented in L_p and s concentrations as the emergent and observable characteristic from the thermodynamics equilibrium of the forces electrostatic resulting force F_1 and the entropic resulting force F_2.

3. Calculations and results

This section may be divided by subheadings. It should provide a concise and precise description of the experimental results, their interpretation, as well as the experimental conclusions that can be drawn. In the context of this work the configurations of the small polyelectrolytes depend only on the parameters *s, N* and *P*. As indicated, we expect a reduction of R_g for increasing s and independently of *P*, both depending on *N* in a different way. Theoretically, we can say that reducing s without crowding, i.e. *P=0%*, may take the polyelectrolyte to different configurations from an ideal rod-like, to a SAW chain and finally to a disperse ellipsoid or spheroid and finally to a compact spheroid. These idealized configurations are related with the scaling exponent ν(s) of equation 10 by ν(s)=3/5=0.6 for a good solvent, ν(s)=1/2=0.5 for a theta solvent and ν(s)=1/3≈0.33 for a bad solvent with the corresponding values of the solvent concentration s. The approximation of a small polyelectrolyte to a spheroid is much better when the solvent is not very good and the number of monomers is not too small.

Figure 2 presents an idealization of five configurations: straight rope-like configuration, SR, almost one-dimensional, ~1D; parabola or horseshoe configuration, Pa, almost two-dimensional, ~2D; sparse spheroid, SS, with dimensionality less than three, <3D, a compact or dense spheroid, DS, three-dimensional, 3D and; the more realistic self-avoiding random walk configuration, SAW, corresponding to a very good solvent with dimension <3D. The SAW configuration is the real optimal configuration for an ideal solvent, providing maximal surface contact with it, and it may have a fractal dimension 2D < fD <3D, which means at the same time the overall volume occupied by the constituent monomers of the polymer and the density or dispersion of occupation of such volume.

With equations 9, 10 and 11 we estimate in three different ways the radius of gyration R_g, and use approximations of the corresponding values of the end-to-end distance $R_{e\text{-}e}$. The consistency and differences between the results at different conditions of s, N and P, allows us to make some interesting hypothesis about the quantitative and qualitative characteristics of the polyelectrolyte configurations and how do they change, and improve the

Preprints (www.preprints.org) | NOT PEER-REVIEWED | Posted: 13 July 2021 doi:10.20944/preprints202107.0309.v1

understanding of the processes performed by the forces F_1 and F_2 in their nonlinear relations described by the $V_{L\text{-}J}$ potential emergent from the conditions defined by the different combination of the parameter values *s, N* and *P*. We estimate R_g with equation 9 for different small pT configurations considering monomers of unit mass and radius.

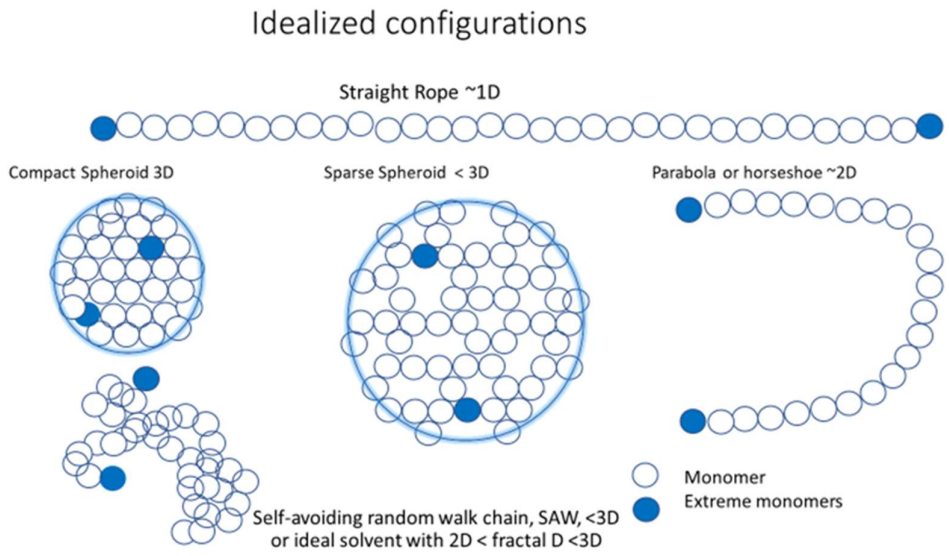

Figure 2. The idealized configurations are simplifications of real configurations, although very small, with a nonzero probability. However, they provide a good base of configurations with qualitative approximations of the main features of symmetry, dimensionality and sparsity of monomers or real polymer configurations. The five idealized configurations considered in this work are: the 3D Dense Spheroid, DS, less than 3D Sparse Spheroid, SS, less than 2D parabola, Pa, 1D Straight Rope, SR, and the Self-Avoiding random Walk, SAW, which in an ideal solvent can become a fractal object with minimal symmetry, dimensionality and density but maximizing the surface contact with the polymer solvent.

Parabola configuration, Pa: For a polymer constituted by N unit length monomers with a 2D symmetric parabola configuration, $y(x)=x^2$, we first find the center of mass given by $x_0 = 0$ and $y_0 = (50/320)b^2 = 0.18b^2$ where b is the end-to-end, $R_{e\text{-}e}$, distance truncated at $y=a$. From the formula to calculate the length L of such segment of the parabola that must be $L=N$, we obtain the increment in the x and y directions, Δx and Δy respectively, when a new monomer is added to the parabola configuration. Then the distance of the N polymer to the center of mass (x_0, y_0) is given by $r_i = ((x_0\text{-}x_i)^2 + (y_0\text{-}y_i)^2)^{1/2}$ where $x_i = x_{i-1} + \Delta x$ and $y_i = y_{i-1} + \Delta y$ with $i = 1,\ldots,N/2$ for N even or $i = 0,\ldots, N\text{-}1/2$ with $r_0 = 0$ if N odd. For such parabola configuration depicted in figure 3, equation 9 gets the specific form:

$$R_g = \left(\frac{1}{N}\left[\sum_{i=1}^{p/2}(2r_i)^2\right]\right)^{\frac{1}{2}} \tag{13}$$

The estimate of the ri depends on the characteristics of the parabola and can be geometrically elaborated. The factor 2 of the r_i appears because of the 2D symmetry of the parabola configuration $y(x)=x^2$ where the unfold length of the polymer is N for N monomers of unitary length and mass.

Preprints (www.preprints.org) | NOT PEER-REVIEWED | Posted: 13 July 2021 doi:10.20944/preprints202107.0309.v1

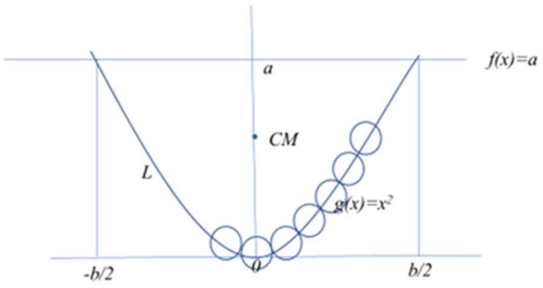

Figure 3. Building a polymer Parabola-like configuration, $y(x)=x^2$, monomer by monomer.

Dense Sphere configuration, DS: in this case equation 9 for R_g can be written as:

$$R_g = \left(\frac{1}{N}[n_1 r_1^2 + n_1 r_2{}^2 + n_1 r_3{}^2 + n_1 r_4{}^2 + \cdots + n_1 r_l{}^2]\right)^{\frac{1}{2}} \quad (14)$$

where $r_i = 2(i-1)r$ for $i=1,2,\ldots, N$ is the distance of the i-th monomer's center to the center of the polymer with a sphere configuration, its center of mass, and n_i is the maximum number of monomers that can fit at such distance from the center in order to have spherical symmetry. It is obtained from dividing the spherical volume occupied by the polymer $V_R = 4/3\pi R^3$ by the spherical volume occupied by one monomer $V_r = 4/3\pi r^3$. With $r=1$ the corresponding values for a spherical symmetric configuration are r1=0 and n1=1, r2=2 and $n_2=7$, $r_3=4$ and $n_3=19$, $r_4=6$ and $n_4=37$,… up to the sum of all $n_i = N$, the total number of monomers. Figure 4 shows the maximum number of monomers by layer of the DS configuration. Then, the maximum number of monomers of radius r that can fit in the polymer volume of radius R is $V_R/V_r = R^3/r^3$ where R increases by units of $2r$. Then, for $r=1$ the maximum number of monomers of each layer are respectively 1, 8-1=7, 27-8-1=18, 64-27-8-1=28, 216-64-27-8-1=116, 1000-116-28-18-7-1=830 and so on.

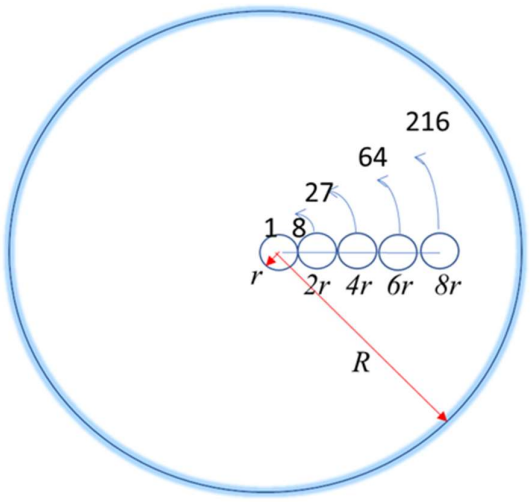

Figure 4. The maximum number of monomers of radius r that fit inside a DS polymer configuration of radius $R = r, 2r, 4r, 6r, 8r, \ldots$

Thus, for the DS we can rewrite equation 9 and equation 14 reduces to, where all $r_i = r = 1$:

Preprints (www.preprints.org) | NOT PEER-REVIEWED | Posted: 13 July 2021 doi:10.20944/preprints202107.0309.v1

$$R_g = \left(\frac{1}{N}[0 + 7(2r)^2 + 19(4r)^2 + 37(6r)^2 + 152(8r)^2 + \cdots + n_l r_l^2]\right)^{\frac{1}{2}} \quad (15)$$

Sparse Sphere configuration, SS: correspond to the same equation 15, but the n_i are smaller than those for DS and the maximum r_i may be larger to fit the same number of monomers tightly packed in a DS configuration. The R_g values for a DS may vary from those very close to the R_g of a DS to those corresponding to a SAW embedded in a spherical volume with very low density of monomers by unit volume.

Ring configuration, Ring: in a ring configuration of radius R of N monomers, all the distances to the center of mass are equal, $r_i = R$ for all $i = 1,\ldots, N$ and R is estimated dividing the perimeter of the ring, $2\pi R$, by the diameter of one monomer, $2r$. Applying equation 9 with $N=19$ and all the $r_i = 6r$ and all the $n_i=1$ for $i=1$ to 19 we obtain $R_g=6r$ and $R_g/N=0.316$, both much larger than the corresponding values for a compact sphere.

Straight Rope, SR, and SAW: the application of equation 9 to SR and SAW are straightforward, in the second case considering the r_i with a random angle and the constraint defined by the projection 1D to be $R_{e\text{-}e}$. In the following tables we present the different results for R_g estimated from the three equations 9, 10 and 12.

In table 3 we present the results of R_g, using equation 10 for polymers of N monomers with stiffness ν(s), for the different values of s from table 1, with the corresponding values of R_h and $R_{e\text{-}e}$ estimated by the approximation of large polymers but depending on salt concentration s. In the indicated conditions the total unfolded length of the polymer is N, and for the DS approximation $R=N^{1/3}$.

In Table 4 are presented the results of the radius of gyration R_g, estimated for SAW with "wormlike chain" model, equation 12, for different persistent lengths L_p, representing the stiffness of the polyelectrolyte: larger L_p corresponds to a stiffer polymer, with effective monomer length normalized to unity. For large polymers, $N \to \infty$, the minimum stiffness, $L_p = l$, gives $R_g \sim (N/3)^{1/2}$, and maximum stiffness $L_p \to N$ gives $R_g \sim N/4$. For small polymers $N \to 1$, maximum and minimum stiffens are about the same and $R_g \sim N/4$.

In Table 5 we present the results of R_g for dense and sparse spheres, DS and SS, parabola, Pa, and straight ropelike, SR, ideal small polymers for the same values of N, estimated as the mean square distance of the monomers to the center of mass, equation 9. The disperse sphere is a sphere with radius $R + r$ where R is the radius of the compact sphere and r is the radius of one monomer.

Table 3. Approximated values of R_g, R_h, $R_{e\text{-}e}$ and R of small polyelectrolytes of $N = 20, 30, 40, 50$ and 60 monomers for different salt concentrations $s = 12.5, 25, 125, 225$ and 525mM. With normalization respect to $A_0(s)$, the Radius of gyration is $R_g = N^{\nu(s)}$ with the corresponding values of ν(s) given in table 1, the hydrodynamics radius $R_h=(5/3R_g)^{1/2}$, the end-to-end distance $R_{e\text{-}e}=3.1R_h$, the total unfolded length $L= N$ and $R=N^{1/3}$ the radius of a compact sphere of N monomers of radius $r=1$.

N		20	30	40	50	60
Measure	[s]=mM, $\nu(s)$					
$R_g = N^{\nu(s)}$	12.5, 0.720	8.8	11.7	14.5	17.0	19.4
	25, 0.700	7.9	10.5	12.8	14.9	16.9
	125, 0.653	7.1	9.2	11.1	12.8	14.4
	225, 0.636	6.5	8.4	10.0	11.5	12.9
	525, 0.607	6.2	8.0	9.5	11.0	12.0
$R_h=(5/3R_g)^{1/2}$	12.5, 0.720	3.8	4.4	4.9	5.3	5.7
	25, 0.700	3.6	4.2	4.6	5.0	5.3
	125, 0.653	3.4	3.9	4.3	4.6	4.9
	225, 0.636	3.3	3.7	4.1	4.4	4.6
	525, 0.607	3.2	3.6	4.0	4.3	4.5

Preprints (www.preprints.org) | NOT PEER-REVIEWED | Posted: 13 July 2021 doi:10.20944/preprints202107.0309.v1

$R_{e\text{-}e}=3.1R_h$	*12.5, 0.720*	*11.8*	*13.7*	*15.2*	*16.5*	*16.6*
	25, 0.700	*11.3*	*13.0*	*14.3*	*15.5*	*16.5*
	125, 0.653	*10.6*	*12.1*	*13.3*	*14.3*	*15.2*
	225, 0.636	*10.2*	*11.6*	*12.7*	*13.6*	*14.4*
	525, 0.607	*10.0*	*11.3*	*12.3*	*13.2*	*14.0*
$R=N^{1/3}$		*2.7*	*3.1*	*3.4*	*3.7*	*3.9*

Table 4. The radius of gyration R_g, estimated with the "wormlike chain model", equation 13, for different persistent lengths L_p, representing the stiffness of the polyelectrolyte: larger L_p corresponds to a stiffer polymer, with effective monomer length normalized to unity. For large polymers, $N \rightarrow \infty$, the minimum stiffness, $L_p = l$, gives $R_g \sim (N/3)^{1/2}$, and maximum stiffness $L_p \rightarrow N$ gives $R_g \sim N/4$. For small polymers $N \rightarrow 1$, maximum and minimum stiffens are about the same and $R_g \sim N/4$.

R_g									
Lp / *N*	*1* *min. stiffness*	*2*	*3*	*4*	*5*	*(N/10)*	*(N/5)*	*(N/2)*	*N* *Max. stiffness*
20	2.4	3.2	3.6	4.0	4.2	(2) 3.2	(4) 4.0	(10) 5.0	5.3
30	3.0	4.1	4.8	5.3	5.7	(3) 4.8	(6) 6.0	(15) 7.3	8.0
40	3.5	4.8	5.7	6.3	6.9	(4) 6.3	(8) 7.9	(20) 9.7	10.5
50	4.0	5.4	6.5	7.3	7.9	(5) 7.9	(10) 9.9	(25)12.0	13.1
60	4.4	6.0	7.2	8.1	8.9	(6) 9.5	(12) 11.9	(30)14.5	13.8

Table 5. R_g for compact and disperse spheres, parabola and ropelike ideal small polymers of *N= 20, 30, 40, 50* and *60* monomers, estimated as the mean square distance of the monomers to the center of mass, equation 9. The disperse sphere is a sphere with radius $R + r$ where R is the radius of the compact sphere and r is the radius of one monomer.

		R_g				
N	*Dense Sphere, DS of aprox* $R=N^{1/3}$	$R=N^{1/3}$	*Sparse sphere, SS*	*Parabola, Pa*	*Straight Rope*	*Ring* $Rg=R=N/2\pi$
20	3.3	2.71	4.7	3.5	11.53	3.2
30	3.8	3.11	5.2	4.5	17.31	4.8
40	4.5	3.42	6.3	5.4	23.08	6.4
50	4.9	3.68	6.6	6.7	28.86	8.0
60	5.3	3.91	9.6	7.0	34.63	9.5

4. Discussion

Authors should discuss the results and how they can be interpreted from the perspective of previous studies and of the working hypotheses. The findings and their implications should be discussed in the broadest context possible. Future research directions may also be highlighted. Table 6 presents a synthesis of the different measures of R_g,

Preprints (www.preprints.org) | NOT PEER-REVIEWED | Posted: 13 July 2021 doi:10.20944/preprints202107.0309.v1

experimental and theoretical as well the corresponding approximations of R_h and $R_{e\text{-}e}$. For the experimental measures of R_g two idealistic extremes are considered. One of very small salt concentration, s=1mM, and another of very large salt concentration, s=10M. These two limits are intended to compare with the idealist configurations DS, SS, Pa and Rope, simulating the stiffness of the polymer by ideal qualities of the solvent that may change the output of the forces F_1 and F_2.

Despite the approximations, idealizations and sometimes strong assumptions of these calculations, the results organized in table 6 offer the opportunity to make some analysis that may help to understand a little more the complexity of the biological fluids. For example, a small polymer DS configuration, N~20, the persistent length must be small, $L_p < 3$, and the equivalent salt concentration must be very high, $s > 10$M. This indicates a compromise between the highest stiffness that a small polymer can have, which is low, and highest stiffness that a solvent can provide, which can be very high or optimal. However, as a nonlinear feedback process, the interplay between the different ranges and intensities of F_1 and F_2 can substantially change the $V_{L\text{-}J}$ and, therefore, its critical points of thermodynamic equilibrium. The possible thermodynamic equilibrium has more alternatives with higher probabilities for larger polymers. However, when the size of the polymer increases and the solvent capacity to soften the polymer is reduced, the results show a tendency of mixed configurations with less symmetry, less spatial density and less homogeneity of the distribution of monomers in space. Thus, the polymer configurations at thermodynamic equilibrium become more diverse and complex, reducing the probability of the more symmetric and compact states, in particular when the temperature is not very low giving energy and instability oscillations to the monomers. For example, for larger polymers, N~60, and very small concentrations of solvent, the configurations tend to correspond more to very sparse SS with tendency to SAW, highly reducing the symmetry and dimensionality of the configuration, corresponding to larger persistent lengths, $L_p > N/5$. These changes of configuration correspond to changes of the forces F_1 and F_2 and their relations, which in its turn generate further changes in the configurations until the thermodynamic equilibrium is achieved. Therefore, theses subtle but important changes on the shape and size of the configurations of the polymers eventually may change competition into complementarity of F_1 and F_2 increasing $R_{e\text{-}e}$ when it is not expected, because the complexity of the entropic forces may transform the expected effects of crowding, $P > 0$, in some particular and specific conditions of solvent and length of the polymer.

Table 6. Comparative organization of the results of R_g estimated from experimental data and theoretical models with the corresponding R_h and $R_{e\text{-}e}$ approximations, for some different polymer lengths and salt concentrations of small polymers constituted by N=20,30,40,50 and 60 monomers of unit length and mass.

N	20		30	40	50	60
Measure	[s]=mM, $\nu(s)$					
$R_g = N^{\nu(s)}$ *Equation 10*	1, 0.794	10.8	14.9	18.7	22.3	25.8
	12.5, 0.720	8.8	11.7	14.5	17.0	19.4
	25, 0.700	7.9	10.5	12.8	14.9	16.9
	125, 0.653	7.1	9.2	11.1	12.8	14.4
	225, 0.636	6.5	8.4	10.0	11.5	12.9
	525, 0.607	6.2	8.0	9.5	11.0	12.0
	1000, 0.592	5.9	7.5	8.9	10.1	11.3
	10000, 0.524	4.8	5.9	6.9	7.8	8.5
R_g	DS	3.3	3.8	4.5	4.9	5.3
	SS	4.7	5.2	6.3	6.6	9.6

Preprints (www.preprints.org) | NOT PEER-REVIEWED | Posted: 13 July 2021 doi:10.20944/preprints202107.0309.v1

Equation 9	*Pa*	*3.5*	*4.5*	*5.4*	*6.7*	*7.0*
	Rope	*11.5*	*17.3*	*23.1*	*28.9*	*34.6*
R_g *Equation 13*	L_p*=1*	*2.4*	*3.0*	*3.5*	*4.0*	*4.4*
	L_p*=2*	*3.2*	*4.1*	*4.8*	*5.4*	*6.0*
	L_p *=4*	*4.0*	*5.3*	*6.3*	*7.3*	*8.1*
	$L_p \approx N/2$	*5*	*7.3*	*9.7*	*12*	*14.5*
	$L_p \approx N$	*5.3*	*8*	*10.5*	*13.1*	*13.8*
$R_h=(5/3R_g)^{1/2}$	*1, 0.794*	*4.2*	*5.0*	*5.6*	*6.1*	*6.6*
	12.5, 0.720	*3.8*	*4.4*	*4.9*	*5.3*	*5.7*
	25, 0.700	*3.6*	*4.2*	*4.6*	*5.0*	*5.3*
	125, 0.653	*3.4*	*3.9*	*4.3*	*4.6*	*4.9*
	225, 0.636	*3.3*	*3.7*	*4.1*	*4.4*	*4.6*
	525, 0.607	*3.2*	*3.6*	*4.0*	*4.3*	*4.5*
	1000, 0.592	*3.1*	*3.5*	*3.8*	*4.1*	*4.3*
	10000, 0.524	*2.8*	*3.1*	*3.4*	*3.6*	*3.8*
$R_{e\text{-}e}=3.1R_h$	*1, 0.794*	*13.1*	*15.4*	*17.3*	*18.9*	*20.3*
	12.5, 0.720	*11.8*	*13.7*	*15.2*	*16.5*	*16.6*
	25, 0.700	*11.3*	*13.0*	*14.3*	*15.5*	*16.5*
	125, 0.653	*10.6*	*12.1*	*13.3*	*14.3*	*15.2*
	225, 0.636	*10.2*	*11.6*	*12.7*	*13.6*	*14.4*
	525, 0.607	*10.0*	*11.3*	*12.3*	*13.2*	*14.0*
	1000, 0.592	*9.7*	*11.0*	*11.9*	*12.7*	*13.4*
	10000, 0.524	*8.8*	*9.8*	*10.5*	*11.2*	*11.7*

Ideally, when *s* is very large and tends to saturation, the stiffness of the polymer tends to be negligible reducing ν towards the lower limit ν(s) > 10M ≈ 1/2 = 0.5 corresponding to an ideal solvent to obtain a polyelectrolyte of maximum softness. The configuration of such polymer strongly depends on temperature and on any tiny physical or entropic force of short, medium or large range. It has strictly L_p*=1* only limited by the hard sphere exclusion of neighbor monomers.

When short range steric, electrostatic, electron clouds exclusion and any other repulsive force are considered, L_p increases and not all the nearest neighbor locations of a monomer are equally probable, F_1 is a short-range repulsion between monomers, including the two extreme monomers being pushed towards the surface of the volume occupied by the polymer, increasing $R_{e\text{-}e}$. Therefore, the stiffness of the polymer is increased, ν(s) ≈ 1M ≈ 3/5 = 0.6 corresponding to an ideal chain or self-avoiding random walk chain, SAW, very soft for long and medium lengths but stiff for short lengths, increasing the persistent length to $L_p > 1$; at such lengths the repulsion of F_1 dominates the contraction of F_2. If this local stiffness is very strong and could propagate to the whole polymer, it would stretch to its maximum extent like a rigid straight rope with $L_p = N$, with N the number of monomers of unitary length. With this configuration the polymer losses all its remaining 3D isotropic symmetry and becomes a 1D straight rope of aligned monomers. In the absence of any other force or thermodynamic perturbation, it can be represented by a total absence of solvent and therefore the maximum stiffness with ν(s ≈ 0) ≈ 1. In this idealized situation

the monomers strongly repel each other stretching the polymer to its maximum length and $Lp = R_{e\text{-}e} = N$, the contour length.

When the polymer is very soft with ideal solvent and the short range steric, electrostatic, electron clouds exclusion and any other repulsive force are dismissed, $F_1 \sim 0$, the complexity of the system allows the emergence and dominance of the packing or agglomeration force as a medium and long-range entropic force relative to the size of a monomer. This tendency formally represented by a force, emerges from the thermodynamic potential generated by the tendency to increase entropy towards configurations with larger probability, those with more equivalent spatial monomer distributions which correspond to the more compacted globular configurations. These configurations are the most symmetric and isotropic, they are fully 3D spatial distributions of monomers occupying a spheroid volume in space. The packing force as one constituent of F_2 is relatively weak and long range but persistent, making the globular configurations inevitable when the other conditions allow. In these configurations the only constrain of the monomers is the directional chemical bonds between neighbor monomers to conform the polymer. By symmetry, isotropy and entropy, the tight globular configurations must have spheroid shape with the extreme monomers tending to the surface of the volume, with an approximated radius $R = N^{1/3}$, obtained from V_p/V_m where $V_p = 4/3\pi R^3$ is the volume of the polymer and $V_m = 4/3\pi r^3$ is the volume of a monomer, respectively with radii R and r, considering $r=1$. In three dimensions, 3D, the spheroid compacity generated by the entropic packing force reduces the persistent length because the angle between nearest neighbors always changes making $L_p < 1$, what can be seen or represented as a further decrease of stiffness of the polymer with smaller ν emulating a much larger salt concentration s, $\nu(s\rightarrow\infty) \approx 1/3 = 0.33$.

The Dense Spheroid, DS, has the maximum symmetry and is fully 3D, the Sparse Spheroid, SS, can have different degrees of sparsity reducing symmetry and dimensionality from 3D up to configurations contained in a 2D disc or even in a ring or incomplete ring with parabola, Pa, or horseshoe-like configuration with dimension even lower than 2D towards a Straight Rope, SR, with minimum symmetry and dimensionality of 1D. The Self-Avoiding random Walk, SAW, is a more real configuration but also more complex and with diverse equivalent and non-equivalent configurations, thus highly probable but difficult to distinguish one specific configurations from others because they may have very similar values for all possible measures. These configurations have a fractal dimension fD where f may be $< 2 < 3$, significantly increasing and even maximizing, even more than the straight rope, the surface contact of the polymer with the solvent. Along with this local configuration of the monomers with their own local stiffness, may be superimposed a global shape such as a parabola or horseshoe configuration with a different global or overall stiffness that may be much more sensitive to F_2, in particular in the direction of changing $R_{e\text{-}e}$ and its relations with R_g and R_h, changing the value of the compression factor $F(s,N,P)$ in equation 1 or equivalently the definition of $\alpha(s,p)$ as $R_g = \alpha\, R_{e\text{-}e}$, just after equation 10. This is all a consequence of a nonlinear feedback process between the forces F_1 and F_2 with the configuration shape of the polymer that they themselves produce in the rich complexity of all possible configurations.

5. Conclusions

This section is not mandatory but can be added to the manuscript if the discussion is unusually long or complex. This work presents a qualitative interpretation of the diversity of small polyelectrolyte configurations using a simple model based on a Lennard-Jones-like potential. These configurations and the corresponding conditions are mostly theoretical idealizations although qualitative realities of the diversity of polymer configurations in a biological fluid. Despite its simplicity, the model allows new hypothesis emerging from the competition and cooperation of electrostatic and entropic forces emerging from the complexity and richness of the interactions of the polymer with the fluid, in particular

the symmetry and dimensionality changes of the configurations. This description gathers new information from different traditional measures of the size of polymer configurations in specified conditions and about the processes towards the thermodynamic equilibrium.

The complexity of a biological fluid generate competition between microscopic and entropic forces producing a rich diversity of polymer configurations that may give the living cell the capacity to perform its living functions. The competition between these two effective forces become synergies in particular and specific conditions generating organization patterns, structures and dynamics with unexpected results such as sudden changes of the effective stiffness of the polymers.

The most important perspective to continue this work is a more quantitative study with the rigor and precision necessary to determine the specific values of the parameters and variables that generate new emergent qualities of the biological fluid and, the corresponding verification and even prediction of experimental measurements.

Author Contributions: Conceptualization, R.M. Gutierrez and G.T. Shubeita; methodology, R.M. Gutierrez and G.T. Shubeita; software, R.M. Gutierrez and J. Guo; validation, R.M. Gutierrez, G.T. Shubeita and C.U. Murade; formal analysis, R.M. Gutierrez and G.T. Shubeita; investigation, R.M. Gutierrez, G.T. Shubeita, C.U. Murade and J. Guo; resources, G.T. Shubeita and C.U. Murade; data curation, C.U. Murade and J. Guo; writing—original draft preparation, R.M. Gutierrez; writing—review and editing, R.M. Gutierrez and G.T. Shubeita; visualization, R.M. Gutierrez and J. Guo; supervision, R.M. Gutierrez, G.T. Shubeita and C.U. Murade; project administration, G.T. Shubeita and C.U. Murade; funding acquisition, R.M. Gutierrez and G.T. Shubeita. All authors have read and agreed to the published version of the manuscript.

Funding: Please add: This research was funded by New York University Abu Dhabi, NYUAD, research projects program in particular the "Faculty Research Fond 78 71202 ADHPG AD312".

Acknowledgments: The authors thank the administrative and technical support of New York University Abu Dhabi, in particular the administrative and logistic officials of the Faculty of Science and Physics Program NYUAD.

Conflicts of Interest: The authors declare no conflict of interest. The funders had no role in the design of the study; in the collection, analyses, or interpretation of data; in the writing of the manuscript, or in the decision to publish the results.

References

1. Klumpp, S., Bode, W. and Puri, P. Life in crowded conditions: Molecular crowding and beyond, *Eur. Phys. J. Special Topics*, Springer Nature, **2019**, pp.1-14.
2. Ellis, R.J. and Minton, E.R.J. Protein aggregation in crowded environment, *Biol. Chem*. **2006,** 387(5), pp. 485-497.
3. Sharp, K. A. Analysis of the size dependence of macromolecular crowding shows that smaller is better, *Biophy. and Compt. Bio*., PNAS **2015**, V. 112, N. 26, pp. 7990-7995.
4. Majumdar, B.B., Ebbinghaus, S. and Heyden, M. Macromolecular crowding effects in flexible polymer solutions, *J Theo. Comp. Chem.*, **2018**, V.17, N. 3, 1840006 1-23.
5. Rivas, G. and Minton, A.P. Macromolecular crowding in vitro, in vivo and in between, *Trends Bio. Sci.,* **2016**, V.41, N. 11, pp. 970-981.
6. Armstrong, K., Wenby, R.B., Meiselman, H.J. and Fisher, T.C. The hydrodynamic radii of macromolecules and their effect in red blood cell aggregation, *Biophys. J*, **2004**, V. 87, 4259-4270.
7. Sim, A.Y.L., Lipfert, J., Herschlag, D. and Doniach, S. Salt dependence of the radius of gyration and flexibility of single-stranded DNA in solution probed by small-x-ray scattering, *Phys. Rev.* **2012**, E 86, pp. 021901 1-5.
8. Smith, S.B., Cui, Y. and Bustamante, C. *Science***, 1996**, 271, 795.
9. Murade, C.U. and Shubeita, G. T. A molecular sensor reveals differences in macromolecular crowding between the cytoplasm and nucleoplasm. *ACS Sensors*, **2019**, 4 (7), 1835-1843.
10. Bohidar, H. B. *Fundamentals of Polymer Physics and Molecular Biophysics*, Cambridge University Press, UK, **2015**.
11. Seol, Y., Skinner, G. M. and Visscher, K. *Phys. Rev. Lett*. **2004**, 93, 118102.
12. Saleh, O.A., McIntosh, D.B., Pincus, P. and Ribeck, N. *Phys. Rev. Lett.* **2009**, 102, 068301.
13. de Gennes, P.G. *Scaling concepts in polymer physics*, Cornell University Press, Ithaca, N.Y. 1979.